INTERNATIONAL JOURNAL OF ADVANCED ENGINEERING AND BUSINESS SCIENCES (IJAEBS)

Journal homepage: https://ijaebs.journals.ekb.eg

Enhancing the performance of Wound-Rotor Self-Excited Induction Generator for Wind Energy Application

Sayed Salama Sayed [a], Soliman M. Sharaf [b], and Fathy M. M. Bassiouny [C]

[a] Department of Electric power and machines, Faculty of Engineering, Helwan University, Cairo, Egypt,

[b] Department of Electric power and machines, Faculty of Engineering, Helwan University, Cairo, Egypt,

[c] Department of Electric power and machines, Faculty of Engineering, Helwan University, Cairo, Egypt,

*Corresponding author: Email address: Sayedsalama494@gmail.com, solimansharaf@yahoo.com, drfbass@hotmail.com

Received: 22-11-2022 **Accepted:** 23-11-2022 **Published**: 01-02-2023

ABSTRACT

One of the main disadvantage of the squirrel cage self-excited induction generator is the variation of both voltage and frequency with the speed variations. The amplitude and frequency of the output voltage of a self-excited induction generator may be adjusted across a wide speed range by using a slip-ring induction machine. In this, paper a study on using a self-excited slip-ring induction generator (SEWRIG) to generate an output with constant voltage and frequency by controlling effective rotor resistance. The steady state characteristics are obtained by analyzing the normalized equivalent circuit of the self-excited induction generator. The study revealed that, for a given stator load impedance, as the speed is varied both the frequency and the voltage can be maintained constant, without changing the excitation capacitance. A closed-loop control scheme for the constant voltage and frequency operation of (SEWRIG) using chopper-controlled rotor resistance is also discussed. With a properly tuned proportional-plus-integral (PI) controller using Particle Swarm Optimization (PSO) algorithm, satisfactory dynamic performance of the (SEWRIG) is obtained. Experiments performed on a 370 W laboratory machine to confirm the feasibility of the proposed method.

Keywords: Induction generators, slip-ring machines, voltage and frequency control.

Nomenclature

F	Per-unit frequency = actual frequency/base frequency.
N	Per-unit speed = rotor speed/synchronous speed.
B	Susceptance per phase.
G	Conductance per phase.
Eg	Air-gap voltage per phase referred to base frequency.
Rs	Stator winding resistance.
Rr	Rotor winding resistance referred to stator side.
Xs	Stator leakage reactance per phase.
Xr	Rotor leakage reactance referred to stator side.
Zl	Load impedance per phase.
Rx	External rotor resistance referred to stator side.
Vt	Stator terminal voltage.
X_c	Reactance of self –excitation capacitor.

1 INTRODUCTION

The self-excited induction generator, (SEIG) is essentially a three-phase induction machine in which the magnetizing current is furnished by capacitor connected across the stator terminals, when it is driven by a suitable prime mover. Voltage build up occurs and electrical power is delivered to the load [1-3]. In recent years, SEIG's have been increasingly used in isolated power system that employ recurrent energy resources, such as be wind energy and hydro power [4-6]. The induction generators are being considered as an alternative choice to well-developed synchronous generator because of their simplicity, ruggedness, little maintenance, low price, brushless (in squirrel cage construction). Although the slip-ring machine is more expensive and requires more maintenance, it permits rotor slip-power control when driven by a variable-speed turbine. When a grid connection is permissible, the slip-ring machine may be operated as a double-output induction generator (DOIG) using the slip-energy recovery technique [7]. In such cases, the voltage and frequency are those of the grid. In autonomous power generation where the grid is not available, a self-excited wound-rotor induction generator (SEWRIG), could be used a fixed voltage and frequency source. In this case, the system cost could be further reduced by the use of a simple rotor resistance controller. Another advantageous feature of the (SEWRIG) is that independent control of the voltage and frequency can be achieved [8-11].

In this paper, a SIMULINK model is built to investigate the voltage and frequency control of a three-phase (SEWRIG) by inserting a controlled external resistance to the rotor circuit. Based on a normalized equivalent circuit model, the frequency and voltage control characteristics are obtained. The experimental results to verify the feasibility of the model as well as the proposed control method are presented.

2 Mathematical Model and Performance Analysis.

Fig. [1] presents normalized equivalent circuit of the three-phase (SEWRIG) where its stator is connected to excitation capacitance required for initiating voltage build up and maintaining the output voltage, while the rotor is connected to an external resistance.

All methods used to determine the steady state performance characteristics of (SEIG) [12-15] based on the analysis of the normalized equivalent circuit adopts either nodal analysis or loop analysis techniques. In the following analysis, we will adopt the nodal admittance method to obtain the mathematical model necessary for the steady state characteristics evaluations. Applying the nodal admittance method to the equivalent circuit yields the following relation:

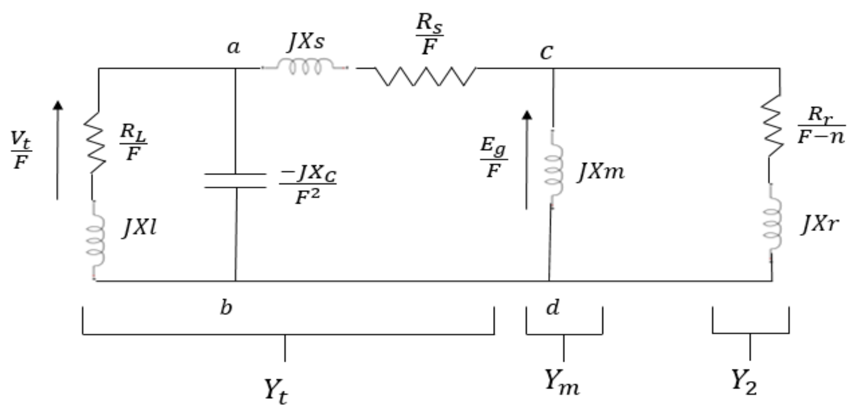

Fig. 1. Equivalent circuit of SEWRIG

$$\frac{E_g}{F}(Y_t + Y_m + Y_{2)} = 0 \quad (1)$$

But, for successful voltage build-up $E_g \neq 0$ which yields:

$$(Y_t + Y_m + Y_{2)} = 0 \quad (2)$$

$$Y_t = \frac{1}{Z_t} = G_t - B_t \quad (3)$$

$$Y_m = \frac{1}{Z_m} = G_m - B_m \quad (4)$$

$$Y_2 = \frac{1}{Z_2} = G_2 - B_2 \quad (5)$$

Where,

$$Z_t = R_t + \mathrm{j}X_t$$

$$Z_m = \mathrm{j}X_m$$

$$Z_2 = \frac{R_r}{\delta} + \mathrm{j}X_r$$

where δ = (F – n)

Equating the real and imaginary parts of the complex equation (2) to zero, the following equations in real numbers are obtained respectively,

$$(G_t + G_m + G_{2)} = 0 \quad (6)$$

$$`(B_t + B_m + B_{2)} = 0 \quad (7)$$

Equation (6) doesn't include the magnetizing reactance and will be solved iteratively to get the self-excitation frequency [13] and (7) can subsequently be used to calculate Xm. The performance analysis and experiments conducted on a three phase , two-poles, 50-Hz, 400 V, 1.62 A, 370W, star connected slip-ring induction machine whose the following equivalent circuit parameters:

Rs=11.5 Ω , Rr=8.03 Ω , Xs=Xr=8.3 Ω , The values of the EMF and magnetization current are both measured by performing the no load test and then these values are used to obtain the polynomials' parameters for the following sixth order polynomial using the Matlab polyval function :

$$E_g = p_1 {I_m}^7 + p_2 {I_m}^6 + p_3 {I_m}^5 + p_4 {I_m}^4 + p_5 {I_m}^3 + p_6 {I_m}^2 + p_7 I_m + p_8$$

$$p_{1=}458.1; p_{2=} - 2796.6; p_{3=}6812.4; p_{4=} - 8321.8; p_{5=}6812.4;$$

$$p_{6=} - 1666.6; p_{7=} - 607.2; p_{8=} - 17.6$$

Figs. [2-3] show the simulated results for the variation of the terminal voltage and frequency characteristics of (SEWRIG) at different values of the external rotor resistance (Rx). It's obvious from figures that increasing Rx has the effect of shifting the performance characteristics to the right-hand side. This indicates that , the same voltage could be obtained at a higher speed by introducing an external resistance to the rotor circuit, the parameters of the machine used in the analysis of Figs. [2-3] are given in reference [14].

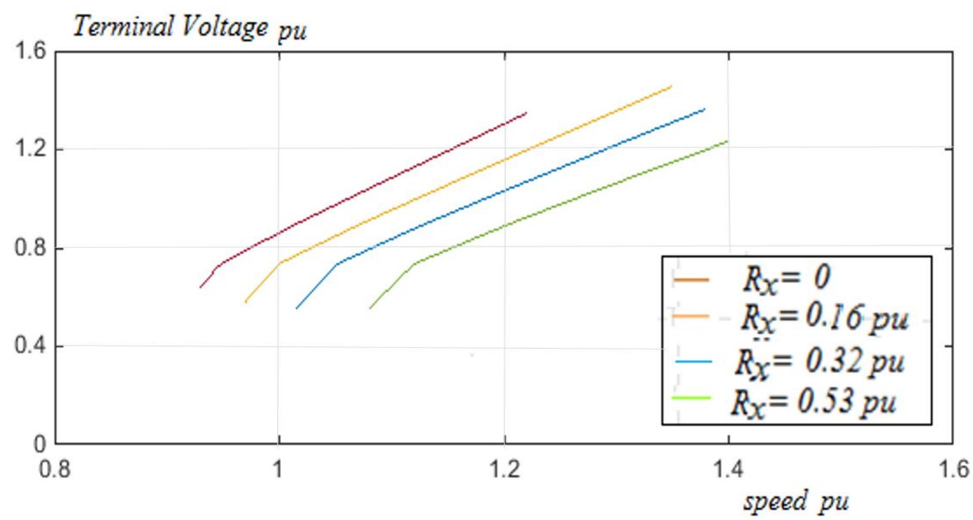

Fig. 2- Stator voltage variation of (SEWRIG) with rotor speed at different values of external rotor resistance.

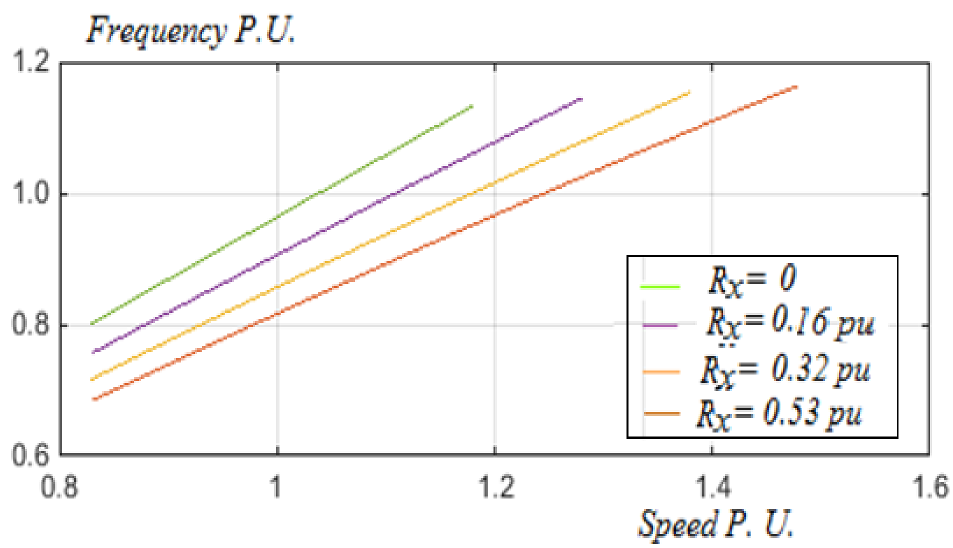

Fig. 3- Frequency variation of (SEWRIG) with rotor speed at different values of external rotor resistance

3 Effect of Rotor Resistance on both Voltage and Frequency

In this section the mathematical model will be modified to deduce the value of the external resistance necessary to keep Either the voltage, frequency, or both at specified value under speed variations. To keep the frequency at fixed value with the speed variation both the load and excitation capacitance are kept constant while the external rotor resistance will vary with the generator speed. From eqn's (5) & (6), the following equation is obtained:

$$G_e + \frac{\delta R_r}{\left(R_r{}^2\right) + \left(\delta R_r{}^2\right)} = 0 \tag{8}$$

Solving Eqn. (8) for δ yields:

$$\frac{R_r}{\delta} = \frac{-1 \mp \sqrt{1 - 4G_e{}^2 X_r{}^2}}{2G_e} \tag{9}$$

For practical induction generators, the term $\frac{R_r}{\delta}$ usually assumes a large negative value because (F-n) is a small negative quantity. Hence, the negative sign in the numerator of (9) should be chosen. Therefore

$$\frac{R_r}{F - n} = \frac{-1 - \sqrt{1 - 4G_e{}^2 X_r{}^2}}{2G_e} \tag{10}$$

Equation (10) shows that, to control the frequency at a given value, the rotor circuit resistance should be change linearly.

By substituting (10) into (7):

$$\frac{1}{X_m} = B_t - \frac{2G_e{}^2\, X_r}{1 + \sqrt{1 - 4G_e{}^2 X_r{}^2}} \tag{11}$$

Equation (11) show that for a given load resistance, excitation capacitance and per unit frequency, the magnetizing reactance Xm is obtained. However an iterative procedure is used to obtain both the magnetizing reactance and the external rotor resistance by employing equations (10) and (11). Once the magnetizing reactance is known the air gap voltage is obtained from the magnetization characteristics. Knowing both magnetizing reactance and the external rotor resistance, the steady-state characteristics of the generator are easily computed.

Fig. [4] shows both the experimental as well as the simulated results of the variation of external rotor resistance required to maintain the frequency at 1 p.u when the load impedance is 4.25 p.u. and the excitation capacitance is 35 μF, while the variation of external rotor resistance required to maintain the frequency at 1 p.u. at a load impedance of 6.9 p.u and an excitation capacitance 35 μF is shown in fig. [5].

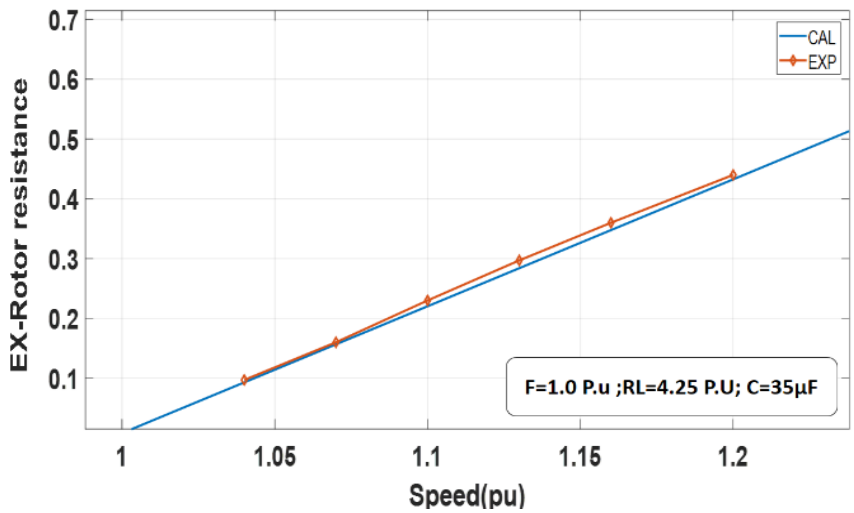

Fig. 4. External rotor resistance Rx for the SEWRIG to operate at rated frequency and rated voltage at Zl=4.25 $p.u$.

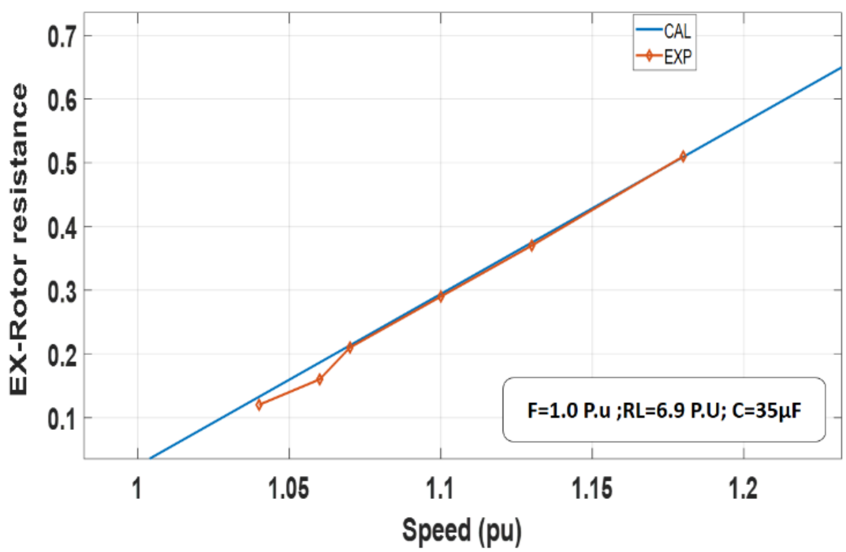

Fig. 5. External rotor resistance R_x for the SEWRIG to operate at rated frequency and rated voltage at Zl=6.9pu.

Fig. [6] shows the realization of the (SEWRIG) for autonomous operations as well as the block diagram of the of the control circuit in its simple form. The visibility of the Simulink model built to simulate the system is tested on the experimental machine described in the previous section by running the voltage build-up process. Fig.[7] presents both the simulated and experimental results for voltage build-up on a 370 W, with excitation capacitor C =35 µF induction machine whose parameters described in the previous section.

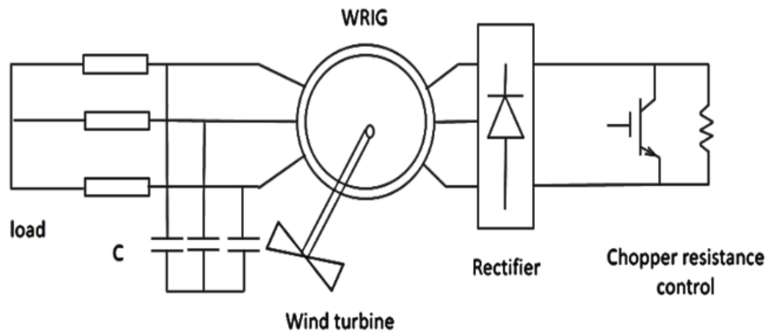

(a) **Circuit diagram**

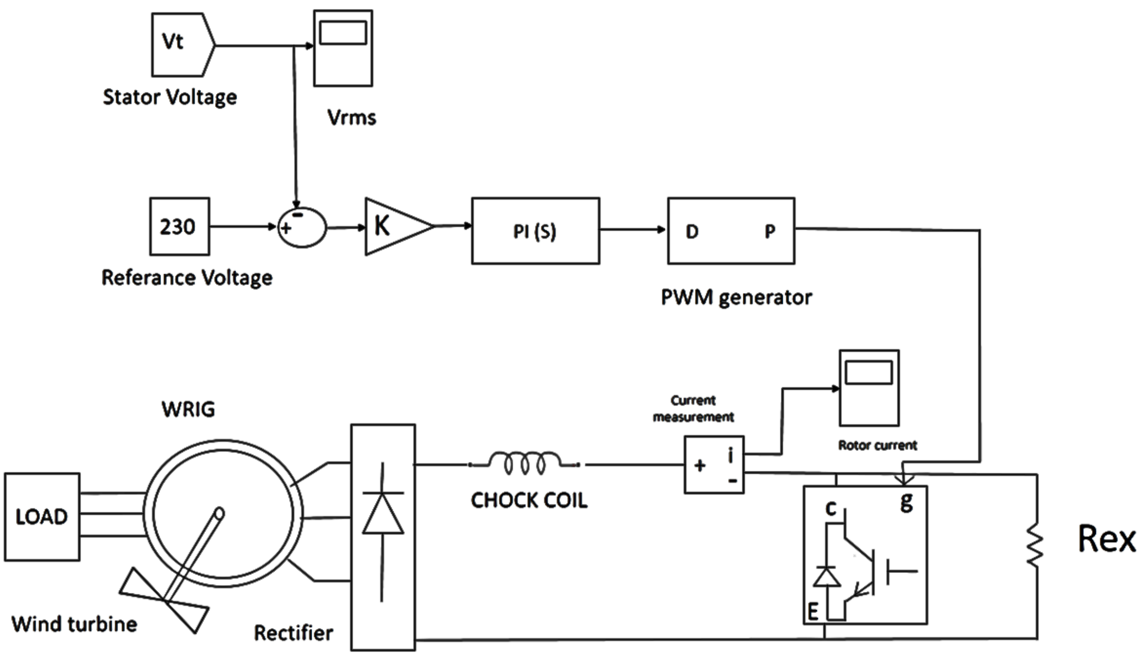

(b) **Control circuit**

Fig. 6. SEWRIG with chopper-controlled rotor circuit resistance.

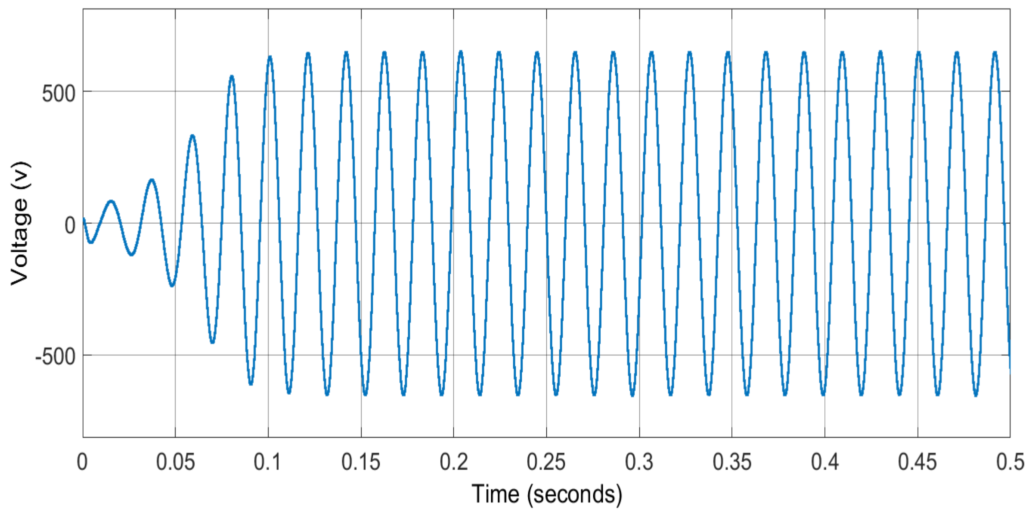

(a) Simulated results

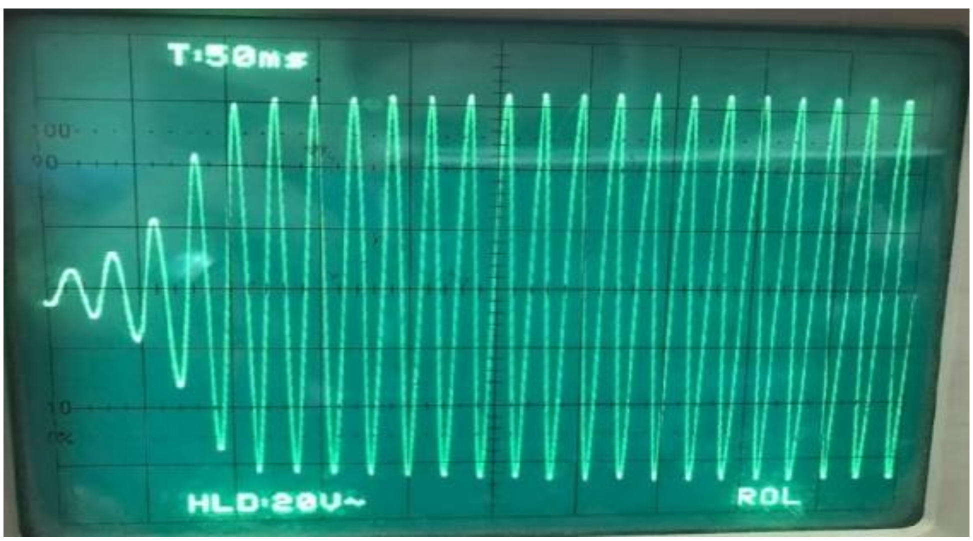

(b) Experimental

Fig. 7. Voltage build-up of SEWRIG at rated speed

Fig. [8] presents both the simulated and measured quantities for the voltage variations when an external resistance of 0.16 pu is inserted in the rotor circuit while the motor speed is kept constant. It is noted that the generated voltage is reduced and this voltage reduction could be retained by increasing the rotor speed. This again insures that the generated voltage could be kept constant when the rotor speed increases by inserting the suitable value of the external resistance to the rotor circuit. The good agreement between the simulated and the experimental results proofs the accuracy as well as the validity of the Simulink model presented in this paper. In the following section the model will be used to simulate the self-regulation of the generated voltage by varying the rotor circuit resistance electronically.

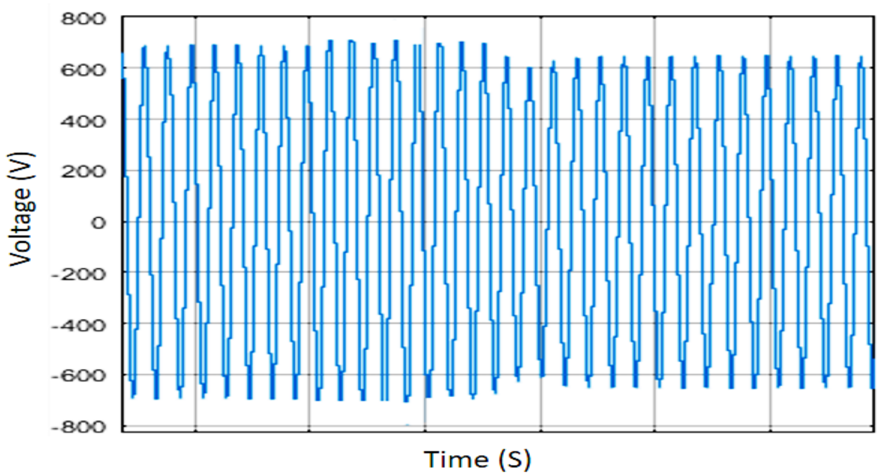

(a) **Simulated**

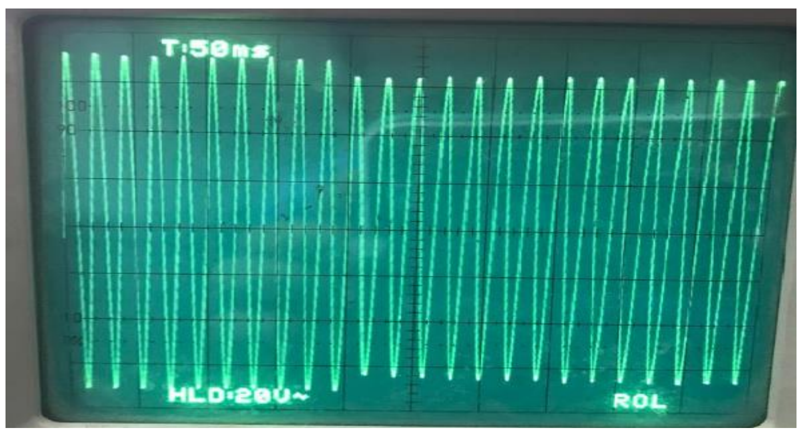

(b) **Experimental**

Fig. 8 Voltage variations of (SEWRIG) after inserting an external resistance to the rotor circuit.

4 Chopper Controlled Rotor Resistance

It is required to have automatic voltage and frequency regulation when the rotor speed changes as in wind generation. By using a chopper-controlled external resistance Instead of a variable three-phase rotor resistance, as shown in Fig.[6-a]. Assuming that the diode-rectifier in the rotor circuit is lossless, the effective external rotor resistance referred to the stator side is given by depends up on the chopper duty cycle as well as square of the stator to rotor turns ratio.

The value of the resistance inserted to the rotor circuit referred to the stator side is given by [15];

$$R_x = 0.5 \times T^2(1 - \mathrm{D}) \times R_{ex} \tag{12}$$

Where,

R_{ex} : the resistance across the chopper.

D : chopper duty cycle.

T : stator to rotor turns ratio.

Equation (12) show that the effective value of the resistance is proportional inversely with the duty cycle D. Figure (6-b) shows the block diagram of the closed loop control circuit to adjust the rotor external resistance based on the desired voltage and the frequency. The stator terminal voltage is considered as the feedback variable because any change in the speed will result in change in the terminal voltage. Referring to figure the measured stator terminal voltage is compared with the reference voltage which represents the desired value of the controlled quantities and then the error signal is fed to the (PI) controller. The output of the PI controller is a signal for controlling the duty ratio (D) of the chopper.

Classical approaches for tuning PID controller gains (such as Ziegler- Nichols (ZN) method) results in high overshoot, and therefore advanced algorithms like Genetic Algorithm (GA) , and Particle swarm optimization (PSO) algorithm are popularly used for enhancing controllers performance[16-17]. In this work, the proposed PI controller's parameters (KPs, KIs) are tuned using PSO algorithm as shown in Fig.9. PSO first produces an elementary swarm of particles in the search space represented by the matrix. Each particle represents a candidate solution to the controller parameters. Emphasis is placed on minimizing the integral time absolute error (ITAE) criterion during the tuning. The controller parameters are determined as follows:

Kp	**Ki**
48.5296	**15.9164**

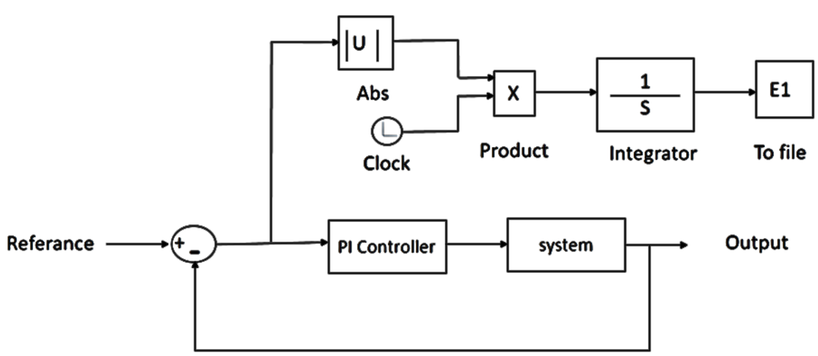

Fig. 9 The cost function used in the particle swarm optimization algorithm.

Figs.[10-13] show the simulated results for the output voltage (peak and rms values) and the frequency subsequent to a speed change from (1.05 to 1.2) pu as shown in fig 13, the load resistance has been kept constant at 4.25 p.u. The PI controller took effect as soon as the speed started to change, outputting a corresponding PWM control signal to increase the rotor circuit resistance and then retain the generated voltage to the previous value. The simulation results for the terminal voltage and frequency corresponding to the speed variations is shown in figs.[10-12]

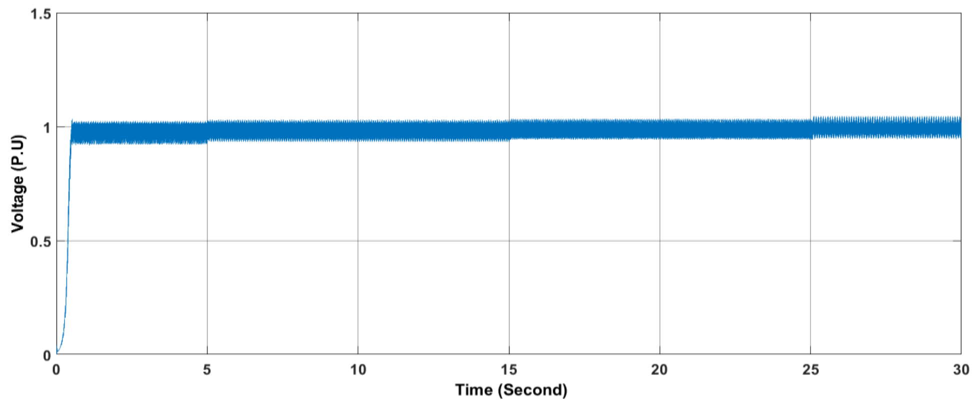

Fig. 10 the simulated rms voltage of (SEWRIG) at Zl=4.25 pu.

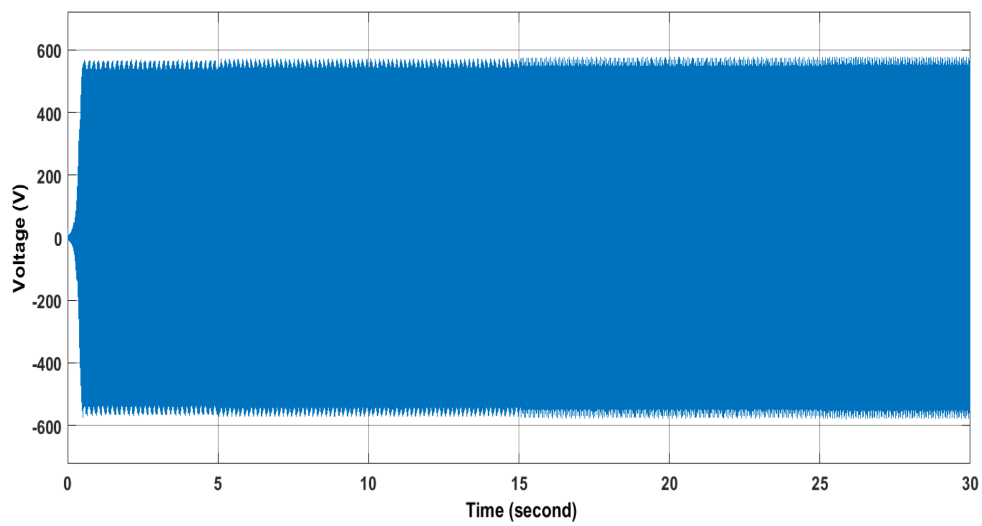

Fig. 11 the simulated peak voltage of (SESRIG) at Zl=4.25 PU.

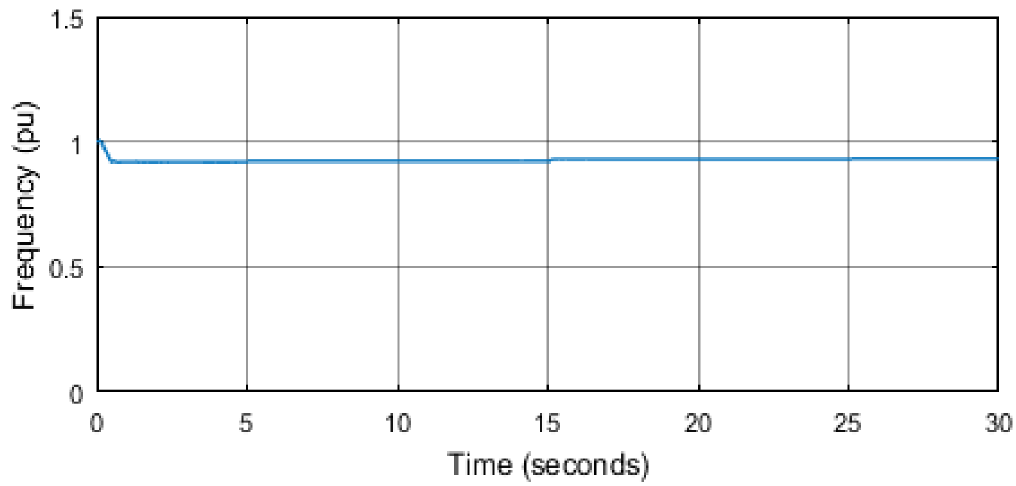

Fig. 12 the simulated frequency of (SESRIG) at Zl=4.25 PU.

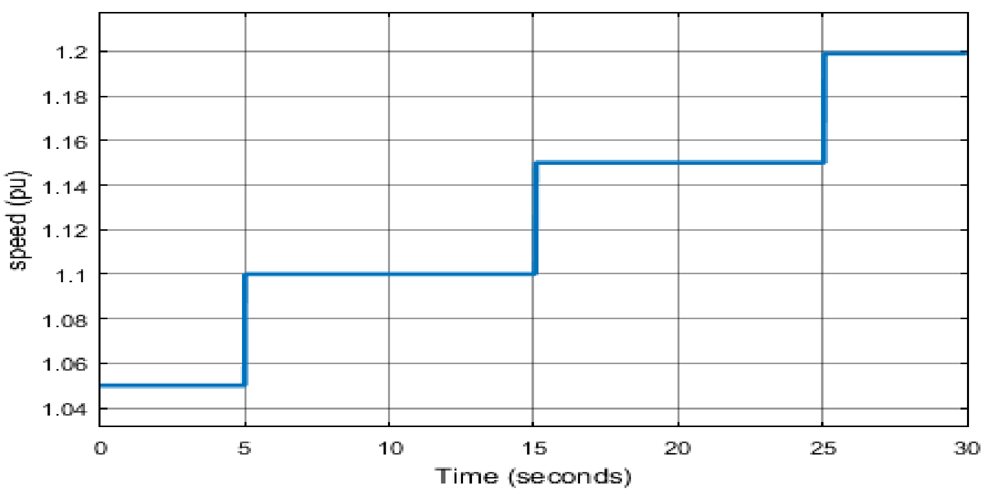

Fig. 13 Speed variation at Zl=4.25 PU.

5 CONCLUSION

In this paper a comprehensive study to model, analyze as well as control the self-excited wound-rotor induction generator (SEWRIG) driven by a wind turbine. A Simulink model has been implemented to simulate the operation of the SEWRIG with an electronically controlled rotor circuit resistance under rotor speed variations. The study showed that the voltage and frequency generated by the SEWRIG could be regulated by introducing an external resistance to the rotor circuit over a wide range of speeds. A Particle swarm optimization (PSO) algorithm is implemented to tune the PI controller properly to obtain good steady-state accuracy and satisfactory dynamic response. The good agreement between the simulated and experimental results proves the accuracy and the validity of the model.

REFERENCES

[1] H. Xiao and F. Liu, A control strategy of DFIG under unbalanced grid voltage, Elect. Ir Electrotechnika 19 (2014) 2828–2836.

[2] Y. K. Chauhan, S. K. Jain and B. Singh, A prospective on voltage regulation of self-excited induction generators for industry applications, IEEE Trans. Ind. Appl. 46 (2010) 720–730.

[3] B. V. Perumal and J. K. Chatterjee, Voltage and frequency control of a stand alone brushless wind electric generation using generalized impedance controller, IEEE Trans. Energy Convers. 23 (2008) 632–641.

[4] L. Wang and D.-J. Lee, Coordination control of an AC-to-DC converter and a switched excitation capacitor bank for an autonomous self-excited induction generator in renew-able-energy systems, IEEE Trans. Indus. Appl. 50 (2014) 2828–2836.

[5] S. A. Deraz and F. E. Abdel Kader, A new control strategy for a stand-alone self-excited induction generator driven by a variable speed wind turbine, Renew. Energy 51 (2013) 263–273.

[6] K. Idjdarene, D. Rekioua, T. Rekioua and A. Tounzi, Performance of an Isolated In-duction Generator Under Unbalanced Loads, IEEE Trans. Energy Conver. 25 (2010) 303–311.

[7] L. A. Lopes and R. G. Almeida, Wind-driven self-excited induction generator with voltage and frequency regulated by a reduced-rating voltage source inverter, IEEE Trans. Energy Convers. 21 (2006Bassiouny, Fathy MM. "Performance analysis of self-excited induction generators." The fourth Saudi technical conference and exhibition (2006): 38-43

[8] Varshney, Lokesh, et al. "Performance characteristics and reliability assessment of self-excited induction generator for wind power generation." IET Renewable Power Generation 15.9 (2021): 1927-1942..

[9] D. Joshi, K. S. Sandhu and M. K. Soni, Constant voltage constant frequency operation for a self-excited induction generator, IEEE Trans. Energy Convers. 21 (2006) 228–234.

[10] D. Joshi, K. S. Sandhu and M. K. Soni, Voltage control of self-excited induction generator using genetic algorithm, Turk. J. Electro. Eng. Comput. Sci. 17 (2009) 87–97.

[11] Shami, T. M., El-Saleh, A. A., Alswaitti, M., Al-Tashi, Q., Summakieh, M. A., & Mirjalili, S. (2022). Particle swarm optimization: A comprehensive survey. IEEE Access.

[12] A. Kheldoun, L. Refou¯ and D. E. Khodja, Analysis of the self-excited induction gener-ator steady state performance using a new efficient algorithm, Electr. Power Syst. Res. 86 (2012) 61–67.

[13] T. F. Chan, “Analysis of self-excited induction generators using an iter-ative method,” IEEE Trans. Energy Conversion, vol. 10, pp. 502–507, Sept. 1995.

[14] Chan, T. F., K. A. Nigim, and L. L. Lai. "Voltage and frequency control of self-excited slip-ring induction generators." IEEE Transactions on Energy Conversion 19.1 (2004): 81-87.

[15] Dubey, G.K., 1989. Power semiconductor controlled drives. Power semiconductor controlled drives.

[16] J. K. Chatterjee, B. V. Perumal and N. R. Gopu, Analysis of operation of a self-excited induction generator with generalized impedance controller, IEEE Trans. Energy Con-version 22 (2006) 307–315H. Xiao and F. Liu, A control strategy of DFIG under unbalanced grid voltage, Elect. Ir Electrotechnika 19 (2014) 2828–2836.

[17] Rahayu, E. S., Ma'arif, A., & Çakan, A. (2022). Particle Swarm Optimization (PSO) Tuning of PID Control on DC Motor. International Journal of Robotics and Control Systems, 2(2), 435-447.